

E. G. Ferreira · F. Fleuret · J.P. Lansberg · N. Matagne ·
A. Rakotozafindrabe

Centrality, rapidity, and transverse-momentum dependence of gluon shadowing and antishadowing on J/ψ production in d Au collisions at $\sqrt{s}=200$ GeV

Received: date / Accepted: date

Abstract We have carried out a wide study of shadowing and antishadowing effects on J/ψ production in d Au collisions at $\sqrt{s_{NN}} = 200$ GeV. We have studied the effects of three different gluon nPDF sets, using the exact kinematics for a $2 \rightarrow 2$ process, namely $g + g \rightarrow J/\psi + g$ as expected from LO pQCD. We have computed the rapidity dependence of R_{CP} and R_{dAu} for the different centrality classes of the PHENIX data. For mid rapidities, we have also computed the transverse-momentum dependence of the nuclear modification factor, which cannot be predicted with the usual $2 \rightarrow 1$ simplified kinematics. All these observables have been compared to the PHENIX data in d Au collisions.

Keywords J/ψ production · heavy-ion collisions · cold nuclear matter effects · RHIC

1 Introduction

At high temperature and densities, QCD predicts the existence of a deconfined state of matter, the Quark-Gluon Plasma (QGP) which is expected to be produced in relativistic nucleus-nucleus (AB) collisions. For thirty years, charmonium production in hadron collisions has been a major subject of investigations, on both experimental and theoretical sides. J/ψ production should indeed be sensitive to the QGP formation, by a process analogous to Debye screening of electromagnetic field in a plasma [1]. A significant suppression of the J/ψ yield was observed at SPS energy by the NA50 experiment [2], and at RHIC by the PHENIX experiment in AuAu [3] and CuCu [4] collisions at $\sqrt{s_{NN}} = 200$ GeV. In 2010 and 2011, data have been taken at the LHC in PbPb collisions at $\sqrt{s_{NN}} = 2.76$ TeV, where the J/ψ has also been found to be suppressed [5, 6, 7].

However, the interpretation of the results obtained in AB collisions relies on a good understanding and a proper subtraction of the Cold Nuclear Matter (CNM) effects which are known to already impact the J/ψ production in proton (deuteron)-nucleus (pA or dA) collisions, where the deconfinement cannot be reached. Experiments on d Au collisions at RHIC [8, 9] have indeed revealed that CNM effects play an essential role at $\sqrt{s_{NN}} = 200$ GeV in the production of J/ψ as well as of Υ (see e.g. [10]). In particular, the shadowing of

Presented at the workshop “30 years of strong interactions”, Spa, Belgium, 6-8 April 2011.

E. G. Ferreira

Departamento de Física de Partículas, Universidad de Santiago de Compostela, 15782 Santiago de Compostela, Spain

F. Fleuret

Laboratoire Leprince Ringuet, École Polytechnique, CNRS/IN2P3, 91128 Palaiseau, France

J.P. Lansberg

IPNO, Université Paris-Sud, CNRS/IN2P3, F-91406, Orsay, France

N. Matagne

Université de Mons, Service de Physique Nucléaire et Subnucléaire, Place du Parc 20, B-7000 Mons, Belgium

A. Rakotozafindrabe

IRFU/SPhN, CEA Saclay, 91191 Gif-sur-Yvette Cedex, France

the initial parton distributions due to the nuclear environment and the nuclear absorption resulting from the breakup of the $c\bar{c}$ pair by its multiple scattering with the remnants of the incident nuclei have a significant impact.

Previous studies [11, 12, 13] have also shown that the J/ψ partonic-production mechanism affects the way to compute the nuclear shadowing and thus its expected impact on the J/ψ production. Most studies on the J/ψ production in hadronic collisions assume that the $c\bar{c}$ pair is produced by a $2 \rightarrow 1$ partonic process where both initial particles are two gluons carrying some intrinsic transverse momentum k_T . The sum of the gluon intrinsic k_T is transferred to the $c\bar{c}$ pair, thus to the J/ψ since the soft hadronisation process does not significantly alter the kinematics. This is supported by the picture of the Colour Evaporation Model (CEM) at LO (see [14] and references therein) or of the Colour-Octet (CO) mechanism at α_s^2 [15]. In such approaches, the transverse momentum p_T of the J/ψ comes *entirely* from the intrinsic k_T of the initial gluons. We will refer to this production mechanism as to the *intrinsic* scheme.

However, this is not sufficient to describe the p_T spectrum of quarkonia in hadron collisions. Recent theoretical works incorporating QCD corrections or s -channel cut contributions have emphasised [16, 17, 18] that the Colour-Singlet (CS) mediated contributions are sufficient to describe the experimental data for hadroproduction of both charmonium and bottomonium systems without the need of CO contributions. For instance, as illustrated by Fig 1, the yield predicted by the LO CSM [19] reproduces correctly the PHENIX, CDF and ALICE measurements without resorting to any colour-octet mechanism nor parameter fitting. Furthermore, recent works [20] focusing on production at e^+e^- colliders have posed stringent constraints on the size of CO contributions, which are the precise ones supporting a $2 \rightarrow 1$ hadroproduction mechanism at low p_T [14].

As a consequence, J/ψ production at low and mid p_T likely proceeds via a $2 \rightarrow 2$ process, which we refer to as the *extrinsic* scheme, such as $g + g \rightarrow J/\psi + g$, instead of a $2 \rightarrow 1$ process. The former $2 \rightarrow 2$ kinematics is then the most appropriate to derive CNM effects at RHIC, and to provide predictions at LHC energy [21, 22]. One could also go further and consider more than two particles in the final state, as expected from the real-emission contributions at NLO and NNLO [16]. It is clear from the yield polarisation [23] that these contributions start to dominate for p_T above $1 - 2m_c$. The effect of more partons in the final state is to increase the difference between the results obtained in both schemes. However the implementation of NLO and NNLO codes in a Glauber model with an inhomogeneous shadowing is not yet available.

In this work, we present our results for the rapidity and transverse-momentum dependence of the nuclear modification factors, R_{dAu} and R_{CP} obtained using the extrinsic scheme for different collision centralities. We compare them with the new PHENIX data [9].

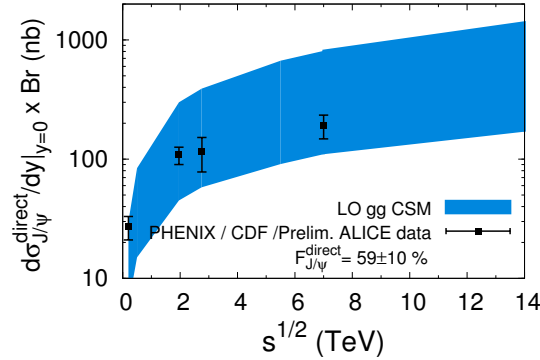


Fig. 1: $d\sigma_{J/\psi}^{\text{direct}}/dy|_{y=0} \times \text{Br}$ from gg fusion in pp collisions for \sqrt{s} from 200 GeV up to 14 TeV compared to the PHENIX [24], CDF [25] and ALICE data [26, 27].

2 Our approach

In order to describe J/ψ production in nuclear collisions, our Monte Carlo framework [11, 12] is based on the probabilistic Glauber model. The nucleon-nucleon inelastic cross section at $\sqrt{s_{NN}} = 200$ GeV is taken to be

$\sigma_{NN} = 42$ mb and the maximum nucleon density to be $\rho_0 = 0.17$ nucleons/fm³. We also need to implement the partonic process for the $c\bar{c}$ production model that allows us to describe the pp data and the CNM effects.

For a given J/ψ momentum (thus for fixed rapidity y and p_T), the processes discussed above, *i.e.* the intrinsic $g + g \rightarrow c\bar{c} \rightarrow J/\psi (+X)$ and the extrinsic $g + g \rightarrow J/\psi + g$, will proceed on the average from initial gluons with different Bjorken- x . Therefore, they will be affected by different shadowing corrections.

In the intrinsic scheme, the measurement of the J/ψ momentum in pp collisions completely fixes the longitudinal momentum fraction of the initial partons:

$$x_{1,2} = \frac{m_T}{\sqrt{s_{NN}}} \exp(\pm y) \equiv x_{1,2}^0(y, p_T), \quad (1)$$

with $m_T = \sqrt{M^2 + p_T^2}$, M being the J/ψ mass.

In the extrinsic scheme, the knowledge of the y and p_T spectra is enough to fix x_1 and x_2 . Actually, the presence of a final-state gluon introduces further degrees of freedom in the kinematics, allowing several (x_1, x_2) for a given set (y, p_T) . The four-momentum conservation explicitly results in a more complex expression of x_2 as a function of (x_1, y, p_T) :

$$x_2 = \frac{x_1 m_T \sqrt{s_{NN}} e^{-y} - M^2}{\sqrt{s_{NN}} (\sqrt{s_{NN}} x_1 - m_T e^y)}. \quad (2)$$

Equivalently, a similar expression can be written for x_1 as a function of (x_2, y, p_T) . Models are then *mandatory* to compute the proper weighting of each kinematically allowed (x_1, x_2) . This weight is simply the differential cross section at the partonic level times the gluon PDFs, *i.e.* $g(x_1, \mu_F) g(x_2, \mu_F) d\sigma_{gg \rightarrow J/\psi + g} / dy dp_T dx_1 dx_2$. In the present implementation of our code, we are able to use the partonic differential cross section computed from *any* theoretical approach. In this work, we shall use the Colour-Singlet Model (CSM) at LO at LHC energy, which was shown to be compatible (see Fig. 1) [17, 19] with the magnitude of the p_T -integrated cross-section as given by the PHENIX pp data [24], the CDF $p\bar{p}$ data [25] and the recent LHC pp data at $\sqrt{s_{NN}} = 7$ TeV [27] and $\sqrt{s_{NN}} = 2.76$ TeV [26].

To obtain the yield of J/ψ in pA and AA collisions, a shadowing-correction factor has to be applied to the J/ψ yield obtained from the simple superposition of the equivalent number of pp collisions. This shadowing factor can be expressed in terms of the ratios R_i^A of the nuclear Parton Distribution Functions (nPDF) in a nucleon belonging to a nucleus A to the PDF in the free nucleon:

$$R_i^A(x, Q^2) = \frac{f_i^A(x, Q^2)}{A f_i^{nucleon}(x, Q^2)}, \quad i = q, \bar{q}, g. \quad (3)$$

The numerical parameterisation of $R_i^A(x, Q^2)$ is given for all parton flavours. Since quarkonia are essentially produced through gluon fusion at RHIC [14], we restrict our study to gluon shadowing. Several shadowing parameterisations are available. Here we will consider three of them: EKS98 [28], EPS08 [29] and nDSg at LO [30]. Recently, a new parameterisation with fit uncertainties, EPS09 [31], has been made available. Yet, in the case of gluons, the region spanned by this parameterisation is approximately bounded by both the nDS and EPS08 values. The central curve of EPS09 is also very close to EKS98. We consider sufficient to use only EKS98, EPS08 and NDSg. The spatial dependence of the shadowing has been included with a shadowing proportional to the local density [32, 33].

The second CNM effect that we take into account concerns the nuclear absorption. In the framework of the probabilistic Glauber model, this effect is usually parametrised by introducing an effective absorption cross section σ_{abs} . It reflects the break-up of correlated $c\bar{c}$ pairs due to inelastic scattering with the remaining nucleons from the incident cold nucleus. Here we choose four values of the effective absorption cross section ($\sigma_{abs} = 0, 2.8, 4.2, 6$ mb) following our previous works [12, 13].

3 Results

3.1 Rapidity and transverse-momentum dependence of R_{dAu}

We first present our results for the *nuclear modification factor* R_{dAu} which characterises the J/ψ suppression in dAu collisions. It is the ratio obtained by normalising the J/ψ yield in dAu collisions to the J/ψ yield

in pp collisions at the same energy times the average number of binary inelastic nucleon-nucleon collisions N_{coll} :

$$R_{dAu} = \frac{dN_{dAu}^{J/\psi}}{\langle N_{coll} \rangle dN_{pp}^{J/\psi}}. \quad (4)$$

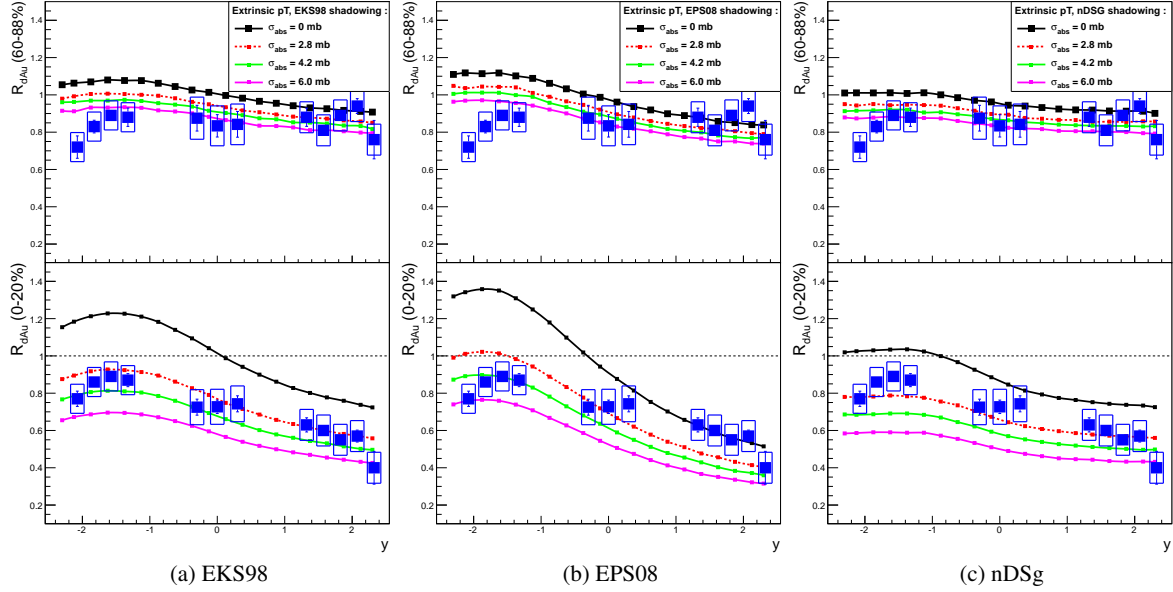


Fig. 2: J/ψ nuclear modification factor in dAu at $\sqrt{s_{NN}} = 200$ GeV for peripheral (upper part) and central (lower part) collisions. The four curves correspond to different values of the effective absorption cross section using different gluon shadowing parametrisations: (a) EKS98, (b) EPS08, (c) nDSg. The data are from PHENIX¹ [9].

In Fig. 2, we show R_{dAu} vs y obtained for different shadowing parametrisations, EKS98, EPS08 and nDSg. We focus only on the extrinsic scheme. Our curves are compared to the PHENIX data [9]. The lower panels in each of Fig. 2 (a), (b) and (c) refer to central collisions (centrality class: 0-20 %, i.e. the 20 % most central collisions) and the upper panels to peripheral collisions (centrality class: 60-88 %). Our previous study [13], based on older PHENIX data [8] suggested that the effective absorption cross section which reproduced the data most accurately was $\sigma_{abs} \approx 3 - 4$ mb. Among the four different values $\sigma_{abs} = 0, 2.8, 4.2$ and 6 mb, which we have been considered here, the best match seems to be between 2.8 and 4.2 mb. The agreement is good for the most central collisions. For peripheral ones, none of the gluon nPDFs which we used is able to accommodate with the most backward data. We also note that the precision of the data does not allow to distinguish between the different shadowing parametrisations. These results show similar features to those Ref. [9], where σ_{abs} is taken to be 4 mb. This was expected since EPS09 shadowing is approximately bounded by EPS08 and nDSg and its central curve is close to EKS98.

We now turn to the discussion of the transverse-momentum dependence of R_{dAu} in the mid-rapidity region. Once more, we would like to emphasize that it can only be predicted if one works in the extrinsic scheme. Our results for different centrality classes for EKS98 are shown on Fig. 3, for EPS08 on Fig. 4 and for nDSg on Fig. 5. R_{dAu} is found to increase with p_T . This is due to the increase of x_2 for increasing p_T which follows from Eq. 2. This effect is more pronounced for the EPS08 than for EKS98 and nDSg due to its stronger antishadowing. Note that the centrality dependence induced by the anti-shadowing – via its strength

¹ Note that the PHENIX points showed here do not include a global systematic uncertainty of $\pm 10\%$ for the peripheral data and of $\pm 8.5\%$ for the central ones.

dependence on the local nuclear density – is increasingly compensated by that of the break-up probability for increasing σ_{abs} . For central collisions, the production point can be well inside the gold nucleus where the anti-shadowing is expected to be stronger but where the break-up probability is also larger.

Our results are also compared to the most recent PHENIX data [34] which suffer from rather large experimental uncertainties for increasing p_T . The agreement with the data is reasonable. In addition to the plot of R_{dAu} vs p_T in the mid rapidity region of PHENIX, we show in the appendix our predictions for backward and forward rapidities to be compared to forthcoming data.

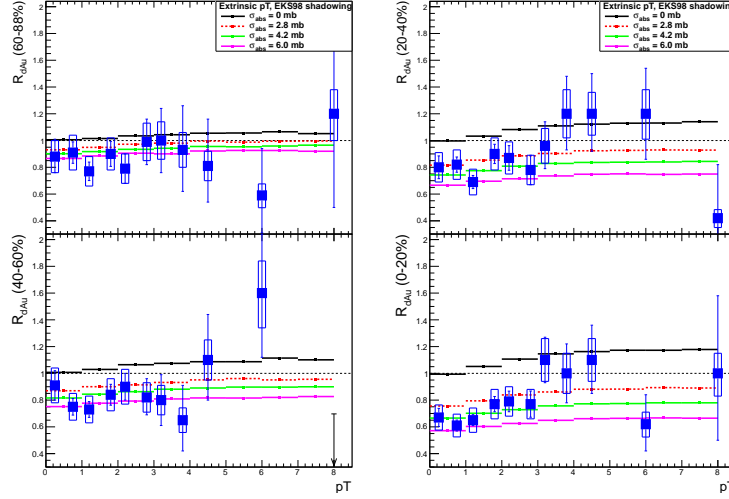


Fig. 3: J/ψ nuclear modification factor in dAu at $\sqrt{s_{NN}} = 200$ GeV vs p_T with $|y| < 0.35$ in different centrality classes for 4 effective absorption cross sections using the EKS98 gluon nPDF.

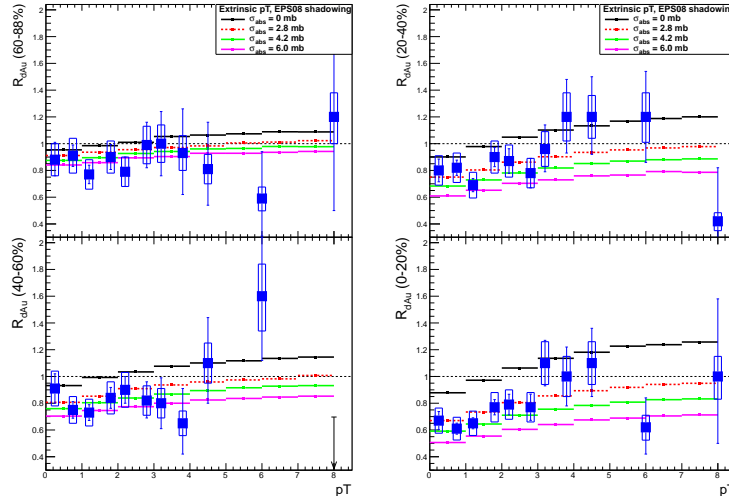


Fig. 4: Idem as the Fig. 3 for EPS08.

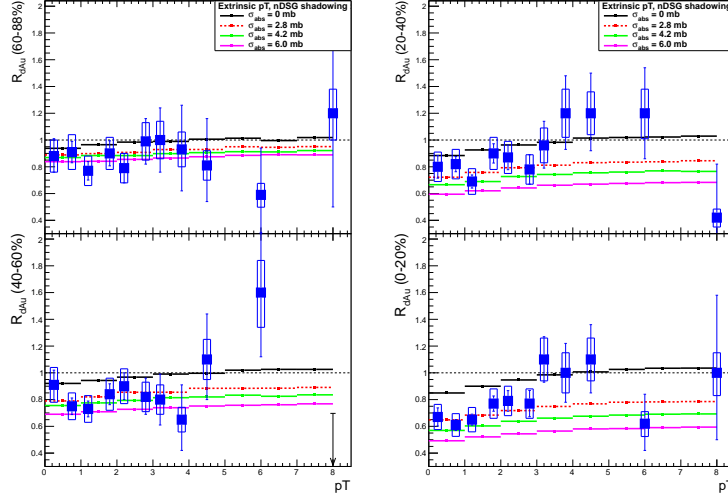


Fig. 5: Idem as the Fig. 3 for nDSg.

3.2 Rapidity dependence of R_{CP}

In this section, we will discuss the rapidity dependence of R_{CP} which give specific information on the centrality dependence of the CNM. This quantity has the advantage to be a ratio in which many of the systematic uncertainties of the data cancel. It is the ratio between central and the peripheral R_{dAu} ,

$$R_{CP} = \left(\frac{\frac{dN_{J/\psi}}{dy}}{N_{coll}^{(0-20\%)}} \right) / \left(\frac{dN_{J/\psi}}{dy} \right)_{(60-88\%)} \quad (5)$$

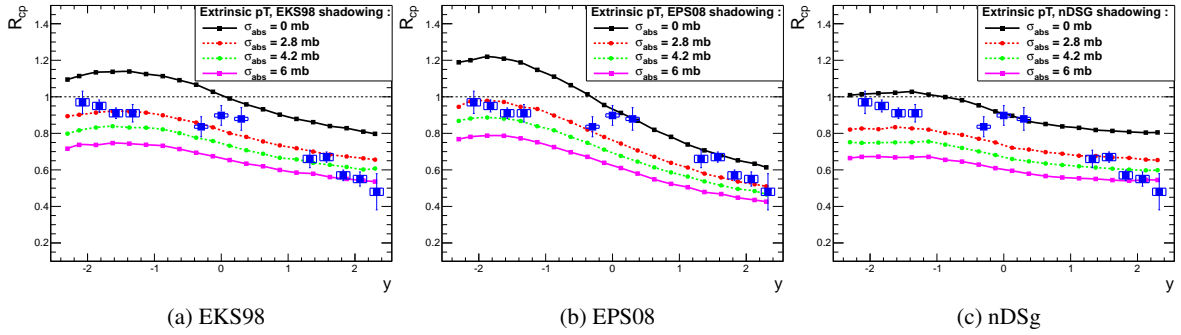


Fig. 6: R_{CP} nuclear modification factor in dAu collisions at $\sqrt{s_{NN}} = 200$ GeV versus y for 4 values of σ_{abs} using: (a) EKS98, (b) EPS08, (c) nDSg. The data are from PHENIX² [9].

Fig. 6 presents our results for R_{CP} versus y for three gluon nPDFs (EKS98, EPS08, nDSg) and the same four values of σ_{abs} as above. We have already discussed the corresponding preliminary data from PHENIX in [13], from which we performed fits of the effective break-up cross section. We had shown at that time that

² Note that the PHENIX points do not include a global systematic uncertainty of $\pm 8.2\%$.

a constant value of σ_{abs} was acceptable when the EPS08 nPDF was chosen. As we obtained in our complete fit [13] taking into account all types of experimental errors [13], the comparison with the published PHENIX data shown on Fig. 6 suggests a σ_{abs} smaller than what would be expected from the comparison with R_{dAu} presented in the previous section. Our curve for EPS08 seems to better reproduce the most forward points, while it slightly misses two of the three mid- y points. A strong shadowing seems in any case needed to account for these data.

4 Conclusions

We have evaluated the rapidity, the centrality and the transverse-momentum dependence of Cold Nuclear Matter effects –essentially the shadowing– on J/ψ production versus rapidity and transverse momentum in dAu collisions at $\sigma_{NN} = 200$ GeV and compared our predictions with the latest PHENIX data. We have used our probabilistic Glauber Monte-Carlo framework, JIN, which allows us to encode $2 \rightarrow 2$ partonic mechanisms for J/ψ production. In particular, we have used the CSM at LO which is now recognised to correctly account for the bulk of the J/ψ cross section in pp at RHIC.

We have used three gluon nPDFs (EKS98, EPS08 and nDSg) and considered a reasonable range of effective absorption cross sections, $\sigma_{abs} = 0, 2.8, 4.2, 6$ mb. Our results, compared to the most recent PHENIX data [9] are in agreement with our previous study [13] where $\sigma_{abs} \approx 3 - 4$ mb was suggested from the comparison with R_{dAu} and $\sigma_{abs} \approx 2 - 3$ mb from the comparison with R_{CP} . This difference may have some physical meaning but the uncertainties both in the knowledge of gluon (anti-)shadowing and in the experimental data preclude drawing any strong conclusions. Finally, we reassess that EPS08 with a strength proportional to the local nuclear density combined with a $2 \rightarrow 2$ partonic process is found to reproduce fairly well the most forward R_{CP} data.

Acknowledgements

We acknowledge the F.R.S.-FNRS (Belgium), the Ministerio de Ciencia (Spain) & the IN2P3 (France) (AIC-D-2011-0740) and the ReteQuarkonii Networking of the EU I3 HP 2 program for financial support. We are very grateful to Darren McGlinchey and Tony Frawley for providing us with the PHENIX experimental points of [34].

References

1. T. Matsui and H. Satz, Phys. Lett. B **178** (1986) 416.
2. M. C. Abreu *et al.*, [NA50 Collaboration], Phys. Lett. B **477** (2000) 28; B. Alessandro *et al.*, [NA50 Collaboration], Eur. Phys. J. C **39** (2005) 335.
3. A. Adare *et al.*, [PHENIX Collaboration], Phys. Rev. Lett. **98** (2007) 232301.
4. A. Adare *et al.*, [PHENIX Collaboration], Phys. Rev. Lett. **101** (2008) 122301.
5. P. Pillot [ALICE Collaboration], J. Phys. G G **38** (2011) 124111
6. C. Silvestre [CMS Collaboration], J. Phys. G G **38** (2011) 124033
7. G. Aad *et al.* [Atlas Collaboration], Phys. Lett. B **697** (2011) 294
8. A. Adare *et al.* [PHENIX Collaboration], Phys. Rev. **C77** (2008) 024912.
9. A. Adare *et al.* [PHENIX Collaboration], Phys. Rev. Lett. **107** (2011) 142301
10. E. G. Ferreira, F. Fleuret, J. P. Lansberg, N. Matagne and A. Rakotozafindrabe, arXiv:1110.5047 [hep-ph].
11. E. G. Ferreira, F. Fleuret, A. Rakotozafindrabe, Eur. Phys. J. **C61** (2009) 859-864.
12. E. G. Ferreira, F. Fleuret, J. P. Lansberg, A. Rakotozafindrabe, Phys. Lett. **B680** (2009) 50-55.
13. E. G. Ferreira, F. Fleuret, J. P. Lansberg, A. Rakotozafindrabe, Phys. Rev. **C81** (2010) 064911.
14. J. P. Lansberg, Int. J. Mod. Phys. A **21** (2006) 3857.
15. P. L. Cho and A. K. Leibovich, Phys. Rev. D **53** (1996) 6203.
16. J. M. Campbell, F. Maltoni and F. Tramontano, Phys. Rev. Lett. **98** (2007) 252002; B. Gong and J. X. Wang, Phys. Rev. Lett. **100** (2008) 232001; P. Artoisenet, J. M. Campbell, J. P. Lansberg, F. Maltoni and F. Tramontano, Phys. Rev. Lett. **101** (2008) 152001; J. P. Lansberg, Eur. Phys. J. C **61** (2009) 693; J. P. Lansberg, J. Phys. G **38** (2011) 124110
17. S. J. Brodsky and J. P. Lansberg, Phys. Rev. D **81** (2010) 051502.
18. J. P. Lansberg, J. R. Cudell and Yu. L. Kalinovsky, Phys. Lett. B **633** (2006) 301; H. Haberzettl and J. P. Lansberg, Phys. Rev. Lett. **100** (2008) 032006.
19. J. P. Lansberg, PoS **ICHEP 2010**, 206 (2010)
20. Z. G. He, Y. Fan and K. T. Chao, Phys. Rev. D **81** (2010) 054036. Y. J. Zhang, Y. Q. Ma, K. Wang and K. T. Chao, Phys. Rev. D **81** (2010) 034015. Y. Q. Ma, Y. J. Zhang and K. T. Chao, Phys. Rev. Lett. **102** (2009) 162002; B. Gong and J. X. Wang, Phys. Rev. Lett. **102** (2009) 162003.

21. E. G. Ferreira, F. Fleuret, J. P. Lansberg, N. Matagne and A. Rakotozafindrabe, Nucl. Phys. A **855** (2011) 327
22. E. G. Ferreira, F. Fleuret, J. P. Lansberg, N. Matagne and A. Rakotozafindrabe, Nucl. Phys. A **862-863CF** (2011) 297 [arXiv:1101.5295 [hep-ph]].
23. J. P. Lansberg, Phys. Lett. B **695** (2011) 149.
24. A. Adare *et al.*, Phys. Rev. Lett. **98** (2007) 232002.
25. D. Acosta *et al.* [CDF Collaboration], Phys. Rev. D **71** (2005) 032001.
26. R. Arnaldi, J. Phys. G **38** (2011) 124106
27. K. Aamodt *et al.* [ALICE Collaboration], Phys. Lett. B **704** (2011) 442
28. K. J. Eskola, V. J. Kolhinen and C. A. Salgado, Eur. Phys. J. C **9** (1999) 61.
29. K. J. Eskola, H. Paukkunen and C. A. Salgado, JHEP **0807** (2008) 102.
30. D. de Florian and R. Sassot, Phys. Rev. D **69** (2004) 074028.
31. K. J. Eskola, H. Paukkunen and C. A. Salgado, JHEP **0904** (2009) 065.
32. S. R. Klein, R. Vogt, Phys. Rev. Lett. **91**, 142301 (2003).
33. R. Vogt, Phys. Rev. C **71** (2005) 054902. M. Bedjidian *et al.*, CERN-2004-009-C, hep-ph/0311048.
34. C. L. da Silva, talk given at “Quark Matter 2011”, Annecy, France (2011).

A Appendix: R_{dAu} vs p_T for different rapidities and centrality classes

In addition to the plot of R_{dAu} vs p_T in the mid rapidity region of PHENIX, we show in this appendix our prediction for backward and forward rapidities.

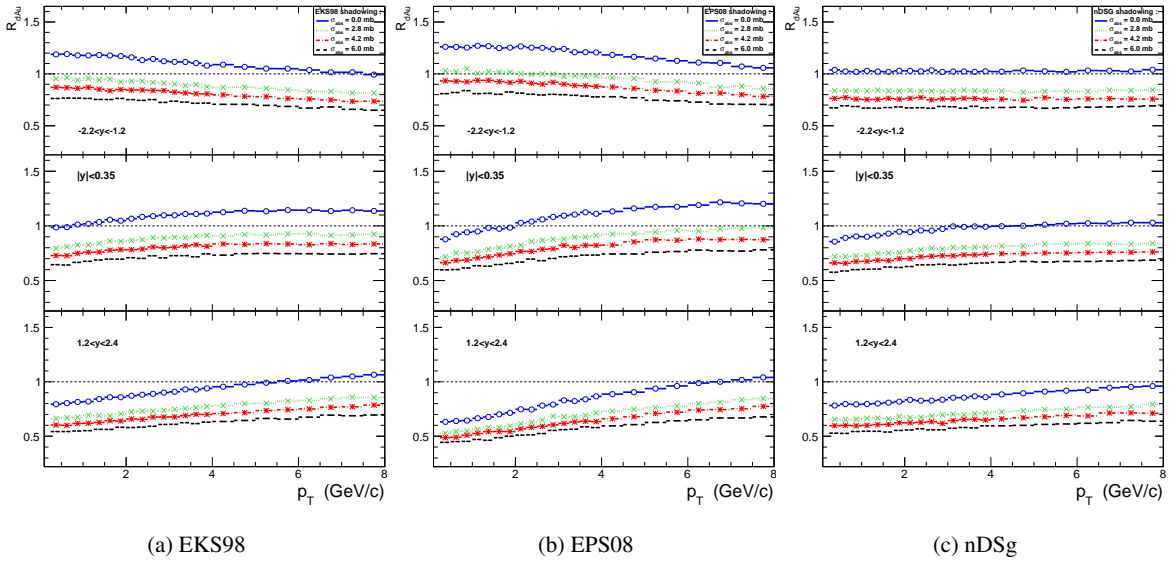


Fig. 7: J/ψ nuclear modification factor in dAu at $\sqrt{s_{NN}} = 200$ GeV vs p_T integrated on the centrality, for four effective absorption cross sections using a) EKS98, b) EPS08, c) nDSg in the 3 rapidity regions covered by PHENIX

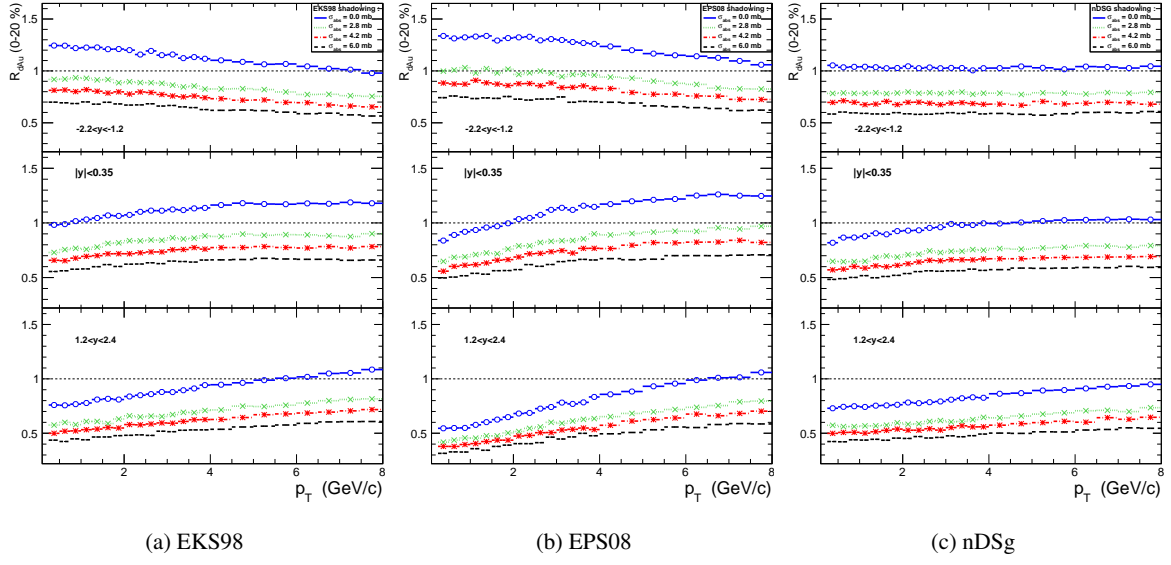


Fig. 8: Idem as the Fig. 7 for the centrality class 0-20 %.

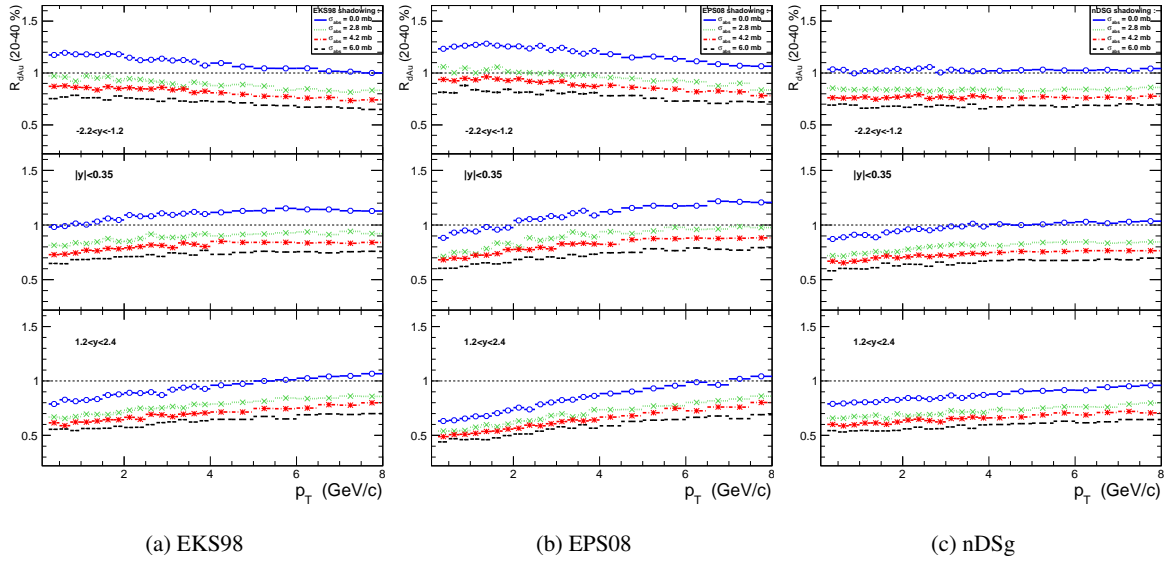


Fig. 9: Idem as the Fig. 7 for the centrality class 20-40 %.

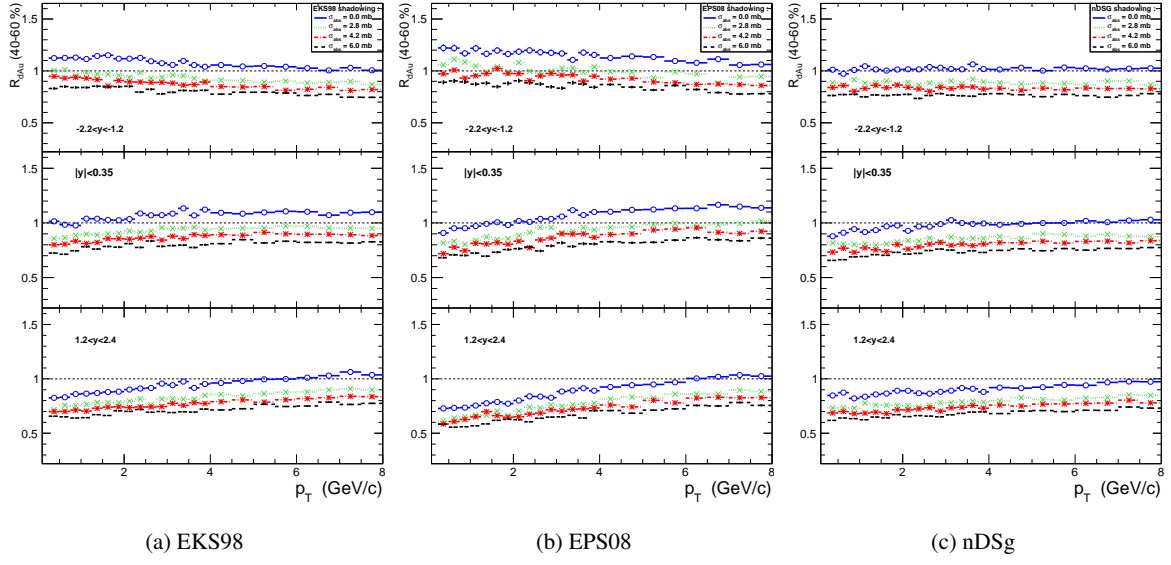


Fig. 10: Idem as the Fig. 7 for the centrality class 40-60 %.

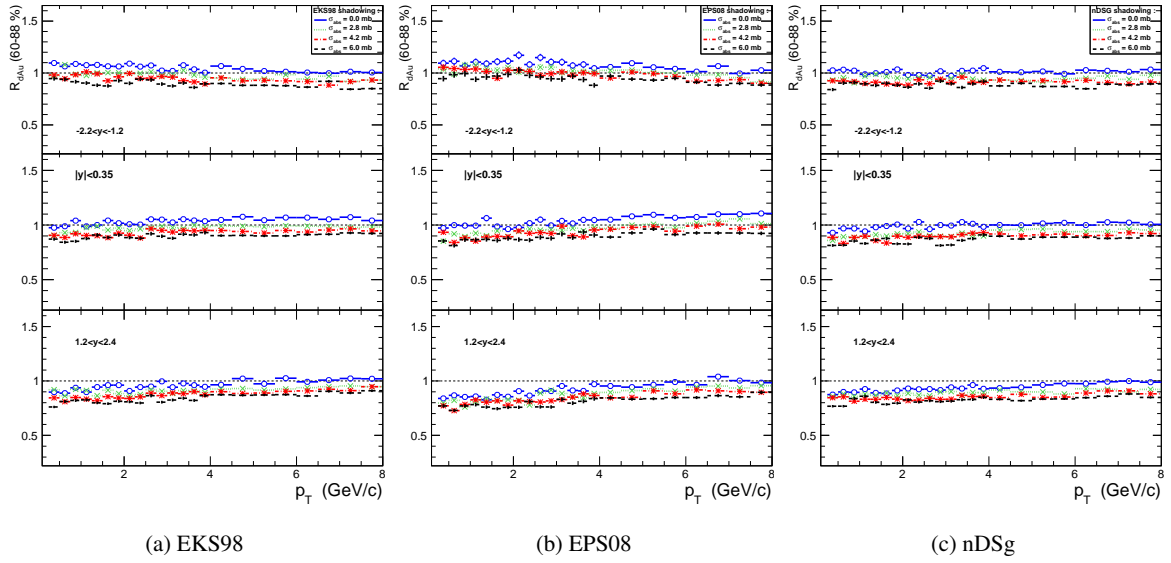


Fig. 11: Idem as the Fig. 7 for the centrality class 60-88 %.